Computational Modeling of Silicate Glasses: a Quantitative Structure-Property Relationship perspective

Alfonso Pedone and Maria Cristina Menziani*

Dipartimento di Scienze Chimiche e Geologiche, Università degli Studi di Modena e Reggio Emilia, Via G. Campi 183, 41125 Modena (Italy)

Corresponding author:

Maria Cristina Menziani
Dipartimento di Scienze Chimiche e Geologiche,
Universita' degli Studi di Modena e Reggio Emilia
Via Campi 183
41125 Modena (Italy)
e-mail: menziani@unimo.it
Tel. +39 059 2055091 Fax. +39 059 3735

Abstract

This article reviews the present state of Quantitative Structure-Property Relationships (QSPR) in glass design and gives an outlook into future developments. First an overview is given of the statistical methodology, with particular emphasis to the integration of QSPR with molecular dynamics simulations to derive informative structural descriptors. Then, the potentiality of this approach as a tool for interpretative and predictive purposes is highlighted by a number of recent inspiring applications.

1. Introduction

Major global challenges in strategic fields such as chemistry, pharmaceutics, medicine, photonics, optics, electronics, clean energy and waste management can be addressed by the development of advanced technologies based on glassy materials. To this goal the correct understanding of the glass structure-property relationships is mandatory, since this is a prerequisite for improving specific

properties and achieve greater focus on end-user application requirements, designing glass compositions for new applications, developing environmentally friendly processes and product, reducing development costs and speed time to market.[1-3]

Notwithstanding the huge improvement in experimental methodologies, like X-ray Absorption Fine Structure, Neutron Diffraction, Nuclear Magnetic Resonance, Infrared and Raman spectroscopy, the elucidation of the glass structure still remain a difficult task.[4] In fact, often difficulties in data interpretation of multicomponent glasses and apparent contradictory structural evidences from different techniques have to be faced.

In this contest, the use of large databases of experimentally measured glass properties [5,6] has facilitated the systematic modelling of glasses and prediction of their properties by statistical analyses of composition-property relationships. However, these tools suffer of important drawbacks: i) the range of compositions studied is determined by presence or absence of the experimental data required; ii) the treatment of glasses of complex compositions involving multiple network formers and modifiers is unpractical; and iii) their objective is exclusively predictive, thus they do not allow a detailed physical understanding for the observed property-composition dependence at the atomic scale.[7,8]

The advent of computational simulation techniques as an accepted component of material development constitutes one of the most important advances in material research. Molecular Dynamics (MD) is nowadays well established as a powerful tool to provide an atomic scale picture of the structure and insight into the behavior of complex glasses in different environments and under different conditions. Recent advances in the interatomic potential for energy functions allow the correct quantitative evaluation of the numerical value of structural, mechanical, thermal, electrical and transport properties for simple glasses.[9-15] However, accurate and reliable evaluation of the same properties for multicomponent glasses has proved far more difficult.

In these cases, i.e. when a direct comparison with experimental observables is not possible, the results of Molecular Dynamics simulations can be used to provide the numerical representation of structure (codified by structural descriptors) to be related with the experimental properties of interest through mathematical models. This imply a shift from empirical composition-property relationships to computational structure-property relationships, thus acquiring an immense practical importance in the development of predictive and interpretative models.[16] This approach, called Quantitative Structure-Property Relationships (QSPR), is well known and extensively apply in the area of drug discovery, and chemical toxicology modeling. However, its application in the field of material design is only recently being explored. [17-19]

In the following a brief overview of the methodology used in QSPR of glasses is given. The mathematical method of choice in relation to the dataset under study is discussed together with the critical role of informative computational-derived descriptors and of appropriate model building and

validation. Then, the potentiality of this approach as a tool for interpretative and predictive purposes is highlighted by a number of recent applications concerning the modeling of density, glass transition temperature, crystallization temperature, leaching, chemical durability, elastic properties, and NMR features. Finally, the future developments that will hopefully improve the QSPR approach described overcoming some current limitations are discussed.

2. Quantitative Structure-Property Relationship analysis.

QSPR methods are based on the hypothesis that changes in the structure are reflected in changes in observed macroscopic properties of materials. The basic strategy of QSPR analysis is to find optimum statistical correlations, which can then be used for a) the prediction of the properties for compounds as yet unmeasured or even not yet synthetized; b) the detailed analysis of structural characteristics that can give rise to the property of interest.

Two very recent reviews provide an in-depth description of the main concepts involved in QSPR modeling of discrete molecules,[20] and materials.[21]Therefore, only a summary of the important elements of the QSPR modeling process in the context of glass design is provided here, underling the basic character of statistical analysis that has been ignored for too long in glass science.

The process of constructing a QSPR model includes the following steps, summarized in Figure 1: 1) selection of a data set; 2) generation of various structural descriptors by means of MD simulations; application of variable selection or/and data reduction methods on the calculated descriptors in order to identify a small subset of these descriptors that are relevant to the macroscopic material properties being modeled (in some cases this step may not be required); 3) generation of linear/multilinear or non-linear relationship between the descriptors and the global material property 4) validation of the model to assess its reliability, robustness, predictivity, and domain of applicability.

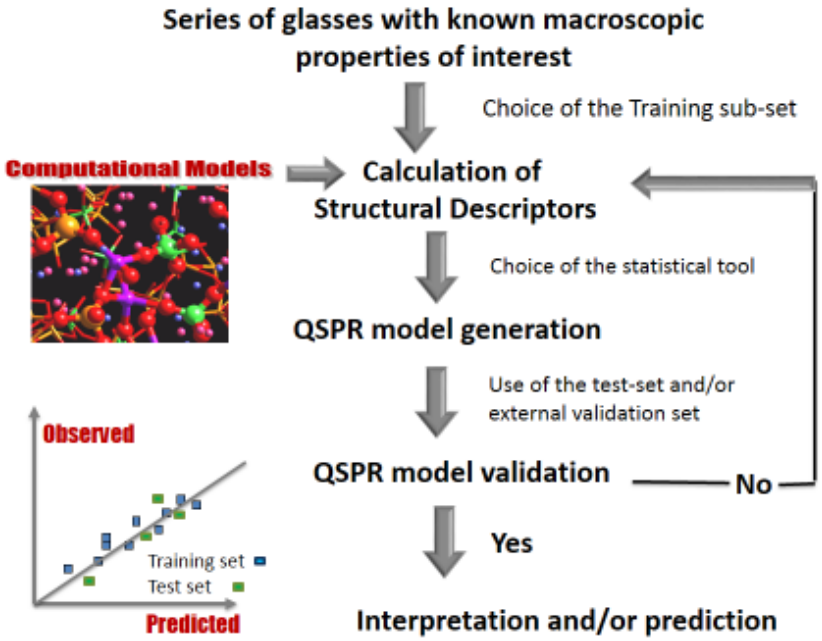

Figure 1. Workflow of QSPR modeling.

2.1 Data set

The key requirement for QSPR modeling is a reliable data set of glasses whose macroscopic properties of interest are known and microscopic structures can be reasonably well-defined by computational simulations. This is termed training data.

The use of heterogeneous experimental data from different sources and laboratories can affect the quality of QSPR models, by increasing the noise in the modeled response, thus affecting the stability and predictivity of models. Other potential obstacle in the development of robust, predictive, and reliable models is the insufficient data size (the range of composition is limited by the occurrence of crystallization, phase separation or other phenomena, or the range of measured property values is too small) and the dependency of the macroscopic property from additional factors besides microscopic structure, such as the history of the material: how it was synthesized, processed, and prepared for testing.

2.2 Structural descriptors

The formulation of informative QSPR models adequate for multicomponent disordered systems is anything but trivial and their predictive and interpretative power depends critically on the information content of the descriptors utilized.[22] The selection of descriptors for meaningful QSPR models implies the knowledge of what features of the structure are measured by a given descriptor and of how the microscopic properties influence the macroscopic (measured) properties in a mechanistic way. Without this knowledge it is hard to apply a "reverse QSPR approach" to optimize materials directly.

To this regard, MD simulations can provide a plethora of promptly available descriptors among which to select the most informative ones. The linear correlation matrix, made up of the correlation coefficients "r" between couples of descriptors, gives an overview of the collinearities existing between them and help in their selections in relation to the statistical model (simple or multilinear regression) of choice and to the interpretation of the properties of interest. The minimal number of orthogonal (not correlated) descriptors of possible relevance to important physicochemical parameters relating to the series of compounds under discussion must be selected for multilinear equations, so that the overall relationships are highly significant by standard statistical criteria.

For oxide glasses, simple descriptors such as average bond lengths, bond angles, coordination numbers, percentage of bridging oxigens (BO) or non-bridging oxigens (NBO) attached to different cations, etc… can be derived from simple statistical averaging or from radial and pair distribution functions and their deconvolution, once the appropriate cut-off distances are defined.[23-25] Others descriptors can be defined as a combination of these ingredients. Finally, useful descriptors of the mid-range structure of the glasses are derived from the Q^n species (Q designates 'quaternary' and n the number of BO oxygens connected to other network former cations), ring size distribution, void size distribution and free volume.[23-27]

2.3 Regression analysis

There is no particular method that is ideal for all problems. The choice of an algorithm should be based on the nature of the data, and also whether the final goal is to build a predictive or interpretative model.

Various statistical methods are nowadays available to build models that describe the empirical relationship between the structure and property of interest. Classical methods, such as single or multiple linear regression (MLR), partial least squares (PLS), neural networks (NN), and support vector machine (SVM), are being upgraded by improving the kernel algorithms or by combining them with other methods, including novel approaches, such as gene expression programming (GEP), project pursuit regression (PPR), and local lazy regression (LLR).[28]

To avoid the risk of "by chance" correlation, statistical models requires significantly more data points than descriptors, since any data set can be fitted to a regression line given enough parameters. For example, in MLR analysis a useful rule of thumb is that the ratio between the number of objects in the data set and the number of descriptors should be at least five to one. Moreover, statistical modelling techniques follow the principle of parsimony postulated by William of Occam and called Occam's Razor (i.e. among a set of equally good explanations for a given phenomenon, the simplest one is the most probable) which means that the models should have as few parameters as possible (i.e. variable is retained in the model only if its removal causes a significant decrease of the statistical parameters compared to those of the current model) and simple explanations have to be preferred than those more complex.

Therefore, according with the number of data point available in the data set, the simple or multiple linear regressions remain as popular choices for QSPR studies of glasses, since they allow an easier interpretation of the phenomena that determine the variation in the observable properties.

The final model built from the optimal parameters will then undergoes validation with a testing set of glasses to ensure that the model is appropriate and useful for prediction and/or interpretation.

2.4 Model Validation

Several procedures are available to determine the reliability and statistical significance of the model. The performance of regression models is commonly measured by the "explained variance" for the response variable y, denoted R^2, and the residual standard deviation (S^2), calculated using the following equations:

$$R^2 = 1 - \frac{\sum(\Delta^2)}{\sum[(\text{Observation} - \text{Average observation})^2]} \quad (1)$$

$$S^2 = \sum(\Delta^2)/DF \quad (2)$$

where, Δ are the model residuals (differences between the experimentally observed and the calculated property values), and DF the degrees of freedom (difference between the number of independent experimental data points and the number of variables including the intercept).

Both statistical parameters provide a measure of how well the model can predict new outcomes, however S^2 is a more robust estimates of the predictive ability of models because, unlike R^2 does not depend on the number of data points in the training set or on the number of descriptors in the model. Good QSPR models have R^2 values close to 1.0 and S^2 values small.

Cross-validation methods are often also applied. This involves omitting in turn one (leave-one-out) or more (leave-many-out) data points from the training

set, generating a QSPR model using the remaining data points, and then predicting the properties of the data point(s) omitted. However, it has often been shown that the use of only this criterion gives an overly optimistic estimate of the predictivity of models is often too optimistic for model validation. [29]

The statistics of prediction of an independent external test set provide the best estimate of the performance of a model. However, the splitting of the data set in training set (used to develop the model) and the test set (used to estimate how well the model predicts unseen data) is not a suitable solution for small-sized data sets and an extensive use of internal validation procedures is recommend.

2.4.1 Outliers For unimodal and symmetrical distributions, data point with deviations at least twice greater than the standard deviation of the data are usually considered outliers. Outliers that cause a poor fit degrade the predictive value of the model; however, care must be taken when excluding these outliers. They can be a clue in incorrectly measured experimental property or in the inadequacy of the model in capturing some important attribute of the material since important microscopic property of the material has not been accounted for in the model and/or the outlier represents an extreme point for this property.

3. Applications of QSPR analysis

Among the examples reported in the literature we focus here on three cases instrumental to demonstrate the achievements of this approach in: a) gaining insight into the physical processes determining the properties of interest (interpretative role of QSPR analysis); b) predicting missing data and optimize property for intended application (predictive role of QSPR analysis); c) assisting in experimental data collection and rationalization and support the design or assessment of foreseen experiments (assisting role of QSPR analysis). These are illustrate in relation to their performances on different properties.

3.1 QSPR Models for Density

Density, one of the most important property in industrial glass production, is perhaps the simplest physical property that can be measured; nevertheless its dependence upon composition is not straightforward. A number of linear expressions, empirically derived by assuming additivity upon components, are available in the literature to predict this property.[30] However, the underlying additivity assumption limited the validity of these equations to narrow ranges of concentration.[31] Moreover, success in the estimation of the density from the chemical composition has been demonstrated only for glasses containing one network former cation (for example Si);[32] corrections by more complex mathematical functions empirically determined from a very large number of

experimental density determinations are necessary for glasses containing two or more network formers and/or intermediate ions, where the linearity assumption fails.[31]

In this context, the successful example of QSPR approach for the prediction and interpretation of density of multicomponent silica-based bioglasses offered by the studies of Linati et al. [33] and Lusvardi et al. [34] is of great significance. In fact, a unique QSPR model derived is able to rationalize the variation of density in four series of glasses made up of three to five different components.

The four series of glasses studied have the following general formula:
Series 1 (KZ): $2SiO_2$•1 Na_2O•1CaO•xZnO (x = 0, 0.17, 0.34, 0.68 mol%); Series 2 (HZ): (2 – y)SiO_2•1 Na_2O•1.1CaO•yP2O5•xZnO (x = 0, 0.16, 0.32, 0.78 mol%; y = 0.10 mol%); Series 3 (HP5Z): (2 – y)SiO_2•1 Na_2O•1.1CaO•yP_2O_5•xZnO (x = 0, 0.16, 0.36, 0.96 mol%; y = 0.20 mol%); Series 4 (HP6.5Z): (2 – y)SiO_2•1 Na2O•1.1CaO•yP_2O_5•xZnO (x = 0, 0.17, 0.36, 0.58 mol%; y = 0.26 mol%);

Among the several structural descriptors derived by MD simulations of the glasses [33, 34] the one which better correlates with the experimental density values is $N_{X\text{-}O\text{-}X}$ /O_{tot}, i.e., the total number of Si-O-Si, Si-O-Zn, Si-O-P, P-O-P, P-O-Zn and Zn-O-Zn bridges found in the simulated glasses normalized for the total number of oxygen atoms (O_{tot}). This quantity represents an overall descriptor of the degree of polymerization of the glass network. The QSPR model obtained is reported in Figure 2a and shows that the density increases with the overall packing degree of the ions in the glasses which is promoted by addition of Zn to the parent glass or substitution of P for Si. This is a not obvious result, since the increase in the density values is the effect of the balance between the variation of the weight of the components and of the molar volume of the different glass compositions.

The statistical soundness of this correlation is confirmed by its ability to a) predict the density values of the training set with an average error of 0.012 g/cm^3); b) predict the density values of two ternary glasses of significant different compositions (TG1:50.6 SiO_2 •42.5 CaO •6.9 ZnO; TG2: 48.6 SiO_2•31.7 CaO•19.7 ZnO) chosen as test set, with a % error comparable to the one obtained for the training set (Figure 2a). Moreover, the QSPR model obtained performs better with respect to the ones obtained by the methods of Priven [35] and Demkina [36] (Figure 2b), especially in the range of high densities (high content of ZnO, more that 0.17 mol%).

Commento [AP1]: Io ho un dubbio che mi porto dietro dai tempi della tesi. Se ho capito bene, il modello correla la densità con il numero di ponti normalizzati rispetto al numero di ossigeno. Questi ultimi dati sono ottenuti dalla dinamica. Se così è quando si vuole usare il modello per predire la densità di vetri di diversa composizione bisogna fare una dinamica molecolare ma questa richiede la conoscenza a priori della densità. Come se ne esce ? Se la densità di partenza è sbagliata vengono sbagliati anche i parametri strutturali (mi ricordo un lavoro di TAndia Adama, quello della corning che aveva costruito un modello per predire la densità sbagliato e quando faceva delle simulazioni MD con i miei potenziali su etri alluminosilicatici con anche il magnesio trovava il magnesio 6 coordinato. Ovviamente era sbagliato e quando glielo feci notare dopo alcuni test mi disse che avevo ragione).
Un metodo potrebbe essere quello di fare una dinamica a P costante ma sappiamo che il vetro scoppia ad alte temperature. Quindi l'unica cosa che si può fare è usare i modelli empirici.
Secondo me la bontà e la potenza del modello si vede dalla correlazione con la Tg …
Un'altra obiezione che potrebbero fare è che non si tiene minimamente conto della natura degli ioni modificatori. Se prendiamo la serie dei vetri contenenti ioni alkalini a pqrità di % di tali ioni il numero di ponti Si-O-Si sono gli stessi ma la densità è diversa perchè le masse cambiano molto quindi quel descrittore strutturale non va più bene. Può essere buono per una serie di vetri binari SiO2-M2O ma se M cambia non va più bene.

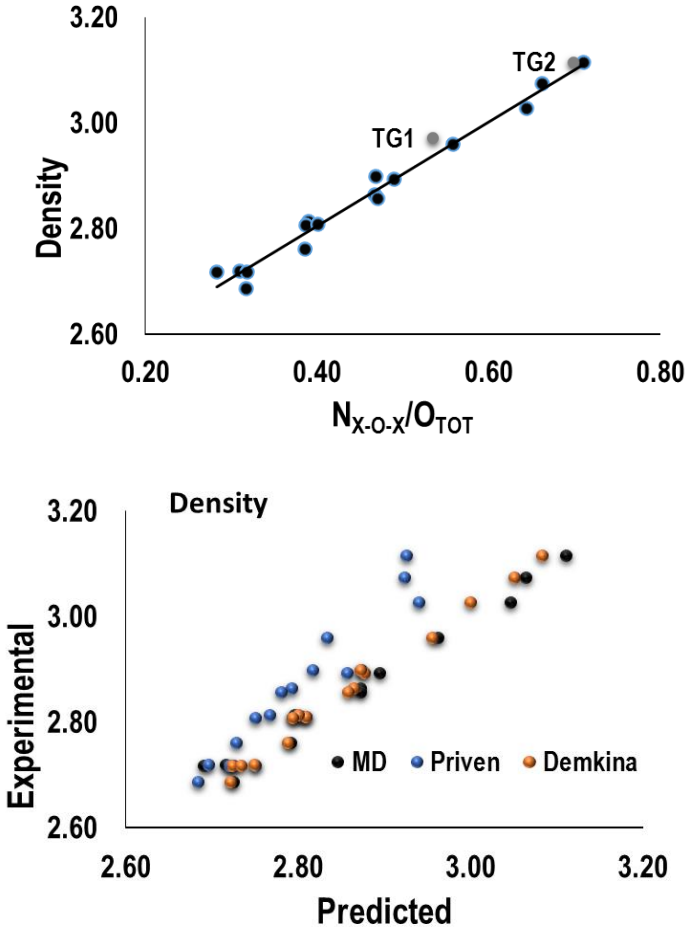

Figure 2. (a) Correlations between the experimental density data values (g/cm^3) and the structural descriptor N_{X-O-X}/O_{tot} of multicomponent glasses.[34] The linear regression obtained is: Density = 0.9873 N_{X-O-X} /O_{tot} + 2.411 n = 16, R^2=0.978, S^2 = 0.012. TG1 and TG2 are used as a test set. (b) Correlations between the experimental density data values and those predicted by means of the N_{X-O-X}/O_{tot} descriptor derived by MD, Priven [35] and Demkina [36] methods. The plots are reproduced by the data values reported in ref. [34].

3.2 QSPR Models for glass transition temperature (T_g) and crystallization temperature (T_c)

The invaluable help that computational techniques furnish in the determination of QSPR models for amorphous materials and the importance of utilizing these models as interpretative tools to gain deep insight difficult to perceive only by the experimental data, is well depicted by the results obtained for complex glasses where two anions are contemporaneously present.[37, 38] In these studies the structural features of Bioactive Fluoro Phospho-Silicate Glasses obtained by classical MD simulations have been used for interpreting the experimental property T_g through a QSPR analysis. The parent compound is the 45S5 Bioglass:[39]
$46.2SiO_2$•$24.3Na_2O$•$26.9CaO$•$2.6P_2O_5$, hereafter named H. The series of glasses studied are: Series 1 (HNaCaF2): $46.2SiO_2$•$(24.3 - x)Na_2O$•$26.9CaO$•$2.6P_2O_5$• $xCaF_2$ (with x = 0, 5, 10, 15, 20, 24.3 mol%); Series 2 ($HCaCaF_2$): $46.2SiO_2$•$24.3Na_2O$•$(26.9 - x)CaO$•$2.6P_2O_5$•$xCaF_2$ (with x = 0, 5, 10, 15, 20, 26.9 mol%); Series 3 and 4 (HZnO and HP5ZnO): $(2 - y)SiO_2$•1 Na_2O•$1.1CaO$•yP_2O_5•xZnO (x = 0, 0.16, 0.32, 0.78 mol%; y = 0.10, 020 mol%); Series 5 (KZnO): Na_2O•CaO•$2SiO_2$•xZnO (x = 0.00, 0.17, 0.34, 0.68 mol%)

The variation of the T_g of silicate glasses upon composition is usually expected to depend on glass polymerization that can be quantified by the Q^n and BO (or NBO) distributions;[40-42] in particular, higher values of glass polymerization is expected to correspond to higher values of T_g. For the series of F-containing glasses analyzed in ref.s 37 and 38, neither of these two descriptors is able to explain the overall decrease of the T_g data values with respect the F-free H glass for the $HCaCaF_2$ series and the decrease up to 15% CaF_2 content for the $HNaCaF_2$ series.

The authors overcome this apparent disagreement by invoking simultaneous structural and energetic modifications of glass network upon F addition and they codified this behavior in the F_{net} descriptor. From a structural point of view, the fluoride ions progressively substitute oxygens in metal coordination with a consequent formation of MF_n ionic moieties, that cause the subtraction of Na and Ca ions from the phospho-silicate matrix. This leads to an increment of the polymerization degree of the phospho-silicate portion of the network (increment of %BO and mean <n> in the Q^n speciation).[43, 44] From an energetic point of view, the interaction of the MF_n ionic zones with the phospho-silicate network at low CaF_2 (CaF_2 <15%) is very weak, being mainly constituted by Na-F neutral pairs, whereas at CaF_2 >15% the MF_n zones are principally made of Ca-F+ pairs which link electrostatically the glass matrix, causing an increment in the strength of the glass network with a consequent increment of T_g values.

The F_{net} descriptor is computed as follow:

$$F_{net} = \frac{1}{N}\left[\sum_{i}^{cations}\sum_{j}^{anions} n_i \cdot CN_{ij} \cdot BE_{ij} \cdot m_{ij}\right] \quad (3)$$

where N is the total number of atoms, n_i is the number of atoms of the i-th species; CN_{ij} is the mean coordination number of ij pairs atoms (i = Si, P, Zn, Na, Ca; j = O2−, F−). BE_{ij} are the bond enthalpies, measured in the gas phase, for each type of bond in the corresponding molecules, as describe in ref. 45. The multiplicative factor m_{ij} represents the maximum number of SiO_4 and PO_4 units linked to the i−O or i−F bonds and is used as fine-tune modulation of the contribution of each bond to the overall network strength.

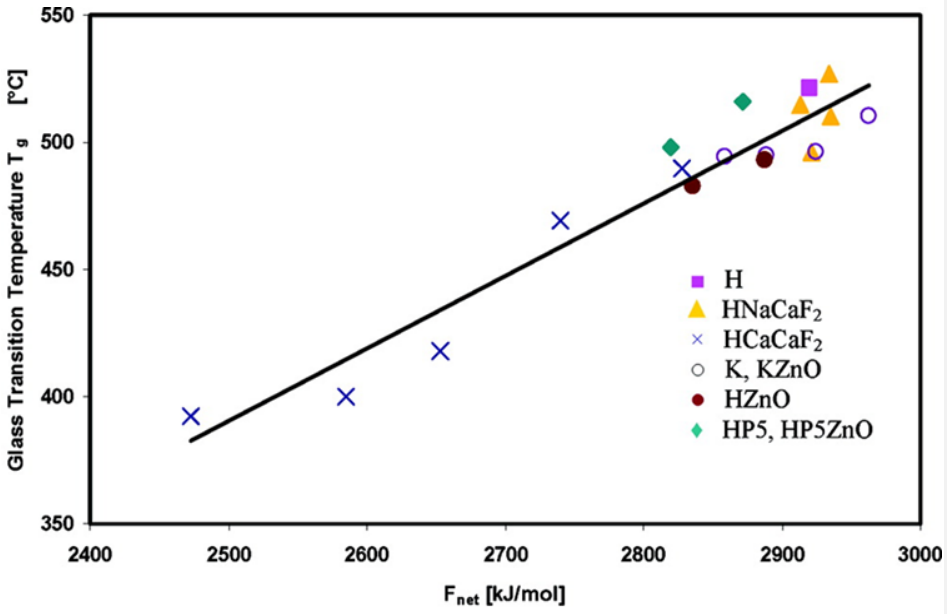

Figure 3. Correlation between experimental glass transition temperature (T_g) and the F_{net} descriptor. The linear regression obtained is: $T_g = 0.2851\ F_{net} - 322.4$, n=18, $R^2 = 0.912$; $S^2 = 8$. reprinted with permission from ref. 37 (*to which refer for details). Copyright 2009 American chemical Society*

The linear correlation obtained between the experimental T_g and the F_{net} descriptor is reported in Figure 3; the positive correlation (slope = 0.2851) accounts for the nature of the T_g measurement that represents the temperature necessary to overcome the flow activation energy. The robustness of the QSPR model is corroborated by the variety of glass compositions covered, which envisages ions with different structural role in the different environment of soda-lime-silicate and phospho-silicate glasses.

The same descriptor F_{net} is able to explains the 68% of the variation in the crystallization temperature (T_c, first peak) of a series of phospho-silicate glasses doped with ZnO, giving a performance comparable with the descriptor $N_{X–O–X}/O_{tot}$, which represents the total number of bridges detected in the three-

dimensional structure derived by MD simulations, and thus accounts for the polymerization of the glass network.[33]

3.3 QSAR models for leaching and chemical durability

The chemical durability of a glass refers to its ability to resist to liquid or atmospheric attacks. The modulation of this physical property of glasses is of fundamental importance in a number of technological area.

Improve durability, i.e. mechanical strength, of glasses would not only enable exciting new applications, but also leads to a significant reduction of material investment for existing applications.[46] However, increasing the durability of a glass by changing its compositions can lead to prohibitively high working temperatures and, therefore, when formulating a commercial glass composition a compromise is made between durability and workability. On the opposite, the dissolution in body fluid is a major part of the functionality of bioactive glasses.[47] These glasses are designed to create chemical gradients which promote, early in the implantation period, the formation of a layer of biologically active bone-like apatite at the interface. Bone-producing cells, i.e. osteoblasts, can preferentially proliferate on the apatite, and differentiate to form new bone that bonds strongly to the implant surface.[48] Glass solubility increases as network connectivity is reduced, consequently, bioactivity occurs only within certain compositional limits and very specific ratios of oxides in the Na_2O-K_2O-CaO-MgO-B_2O_3-P_2O_5-SiO_2 systems.[49]

The physico-chemical requirements for biocompatibility and bioactivity in terms of compositional limits and role of additional ions in tailoring new important mechanical and biological properties for specific clinical applications [39] are poorly known at present. In the following we show, by summarizing the results of two case studies, how sound relationships among the structural role of some key elements that appear to control bioactivity can by established and exploit for rational glass design.

3.3.1 Zinc-containing bioglasses

Zinc added to bioglasses improve their chemical durability, mechanical properties and endows antimicrobial activity; moreover, the release of small concentration of zinc incorporated into an implant material promotes bone formation around the implant and accelerates recovery of the patients, improve adhesion of denture adhesives, etc… Still, it is important to control the Zn releasing rate in order to prevent adverse reactions and to optimize the glass composition to reduce glass degradation without affecting the hydroxyapatite deposition.

The first example of a complete cycle in rational glass design has been reported for these glasses, and is summarized in Figure 4. The authors [33, 50] derived the ratio of Zn/P concentration which produces an optimal dissolution in the body fluid in order to maintain the bioactivity. The QSPR model used accounts for the role of network polymerization on water chemical durability: $\Sigma\%X_i = -1.92\ N_{X\text{-}O\text{-}X}/O_{tot} + 1.33$, n= 6, $R^2 = 0.865$, $S^2 = 0.12$, where is $\Sigma\%X_i$, is the total leaching of the glass constituent and the $N_{X\text{-}O\text{-}X}/O_{tot}$ descriptor has been described in the previous paragraph. The number of data point in the data set is small, nevertheless the content of information of the descriptor chosen suggests that solubility is hindered by the zinc tendency to copolymerize with the Si tetrahedral, manifested by a significant increasing of the total number of X-O-X bridges detected in the glass. This model explains the slow rate of zinc dissolution into the media and provides insights into the overall reaction rate reduction of the zinc-containing glasses, regulated by the progressive reduction of the number of NBO species, which ensure the presence of large channels for alkali migration in the network and rapid exchange of Na^+ with H_3O^+ at the glass surface, as summarized by the following linear regressions: $\%P_{(released)} = 0.009\ \%P{-}NBO - 0.46$, n=6; $R^2 = 0.93$, $S^2 = 0.03$; $\%Na_{(released)} = 0.007\ \%Na{-}NBO - 0.32$, n=6; $R^2 = 0.74$, $S^2 = 0.12$; $\%Ca_{(released)} = 0.006\ \%Ca{-}NBO - 0.35$, n=6; $R^2 = 0.84$, $S^2 = 0.03$; where %P−NBO, %Na−NBO, and %Ca−NBO are the percentages of NBOs bonded to P, Na, and Ca ions.

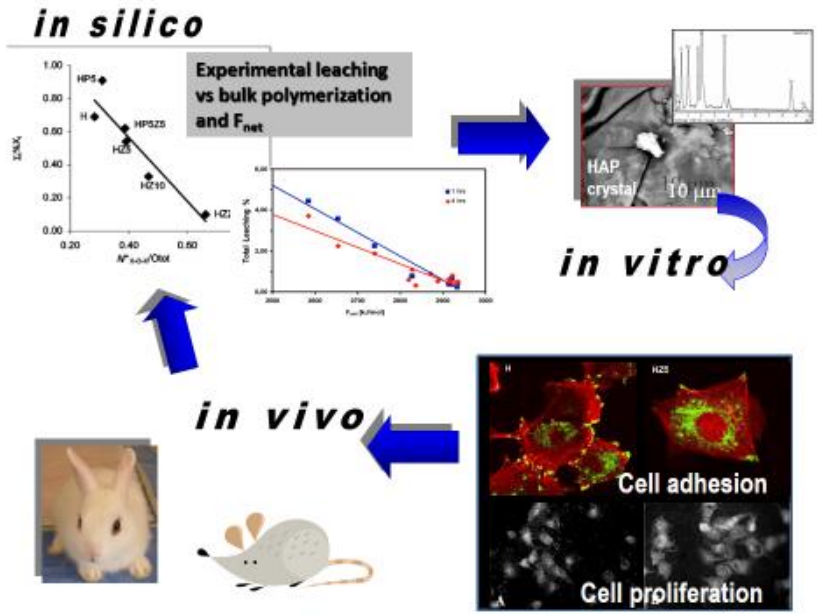

Figure 4. The rational glass design cycle illustrated for Zn-containing Bioglasses [33, 50-53]

The results of the QSPR study (*in silico* study) indicated the HZ5 and HP5Z5 as candidates for further studies. Chemical durability tests in water and *in-vitro* observations in acellular medium [51, 52] confirmed that the HZ5, HP5Z5, but also the HP5Z10 glasses manifest the pre-requisite for bioactivity, since they are able to form a HA layer on their surface after soaking in SBF solution. Moreover, the results of cell culture tests with MC-3T3 osteoblast cells and related cytotoxicity tests allow the selection of the HZ5 and HP5Z5 glasses (not HP5Z10) as the ones with optimal ratio of Zn/P to maintain cell adhesion and cell growth comparable to the parent bioglass (H) used as a control. Finally, *in vivo* behavior performed on the HZ5 glass [53] matches that in vitro perfectly; they show comparable glass degradation processes and rates, ruled by the amount of zinc in the glass.

These findings triggered furthers investigations on the chemical durability (express as total leaching % detected after different immersion time in bi-distilled water) of Phospho-modified bioglasses which has been rationalized by means of the F_{net} descriptor defined in the previous paragraph (equation 3).[37] The linear correlations obtained after 1 and 4 h of soaking are: Tot.Leach.% = -0.01156 x F_{net} + 34.11; n=9; R^2=0.965; S^2=0.020, and Tot.Leach.% = -0.00808 x F_{net} + 23.99; n=13; R^2=0.851; S^2=0.105, respectively (Figure 4). It is worth noting that the correlation coefficients decreases as a function of immersion time (R^2 = 0.965, 0.851, 0.682 and 0.640 after 1, 4, 24, 96 hours) due to the occurrence of precipitation processes that cannot be taken into account by the F_{net} descriptor. The negative slope of the correlations indicates that the higher F_{net} (i.e. the overall strength of the glass network), the greater the chemical durability.

It is worth noting that the wide range of variation of the correlations is essentially due to the glasses of the $HCaCaF_2$ series (Total Leaching %: 0.77-4.44 mol%, 1hrs) which show much higher solubility with respect to the HNaCaF2 series (Total Leaching %: 0.37-0.24 mol%, 1hrs). This behavior has been ascribed by the authors [37] to the conversion of Ca^{2+} and Na^{+} species to $Ca{-}F^{+}$ and NaF ones upon addiction of the fluorine ions with an overall reduction of network complexation.

3.3.2 Yttrium-containing aluminosilicate glasses

A key requirement for successful application of glass delivery systems for radiation is a high durability of the glass used to minimize the release and the fatal results of circulation of the radioactive agent in the body. Therefore, also in this case a deep understanding of the way in which the glass composition controls the glass dissolution is needed.

In a recent work by Christie et al.[54] the specific structural features of the glasses that control the solubility of a series of yttrium aluminosilicate glasses (parent glass composition: $17Y_2O_3$-$19Al_2O_3$-$64SiO_2$) have been extracted from MD simulations and used to predict the solubility of these materials. In particular, a linear combination of the following descriptors showed a high correlation with the experimental solubility: 1) CN_{SiOSi}, which is the average O–Si coordination number of oxygen atoms already coordinated to at least another silicon atom. This count for the connectivity of the silicon atoms in the network; 2) the yttrium clustering ratio R_{YY} using the ratio of the measured Y–Y coordination number (at a cutoff of 5 Å) to the number expected if the yttrium atoms were distributed uniformly (randomly) throughout the available space.[55] Values of $R_{YY} > 1$ denote spatial clustering, while $R_{YY} = 1$ describes a uniform distribution of Y atoms throughout the available space; 3) number of intratetrahedral O–Si–O bonds per yttrium atom (N_{intra}). In general, any increase in the amount of intratetrahedral Y–O coordination will decrease the number of fragments of the glass network coordinated to yttrium. Because the strong Y–O interaction can be expected to reduce the mobility and increase the resistance to dissolution of these fragments, a positive correlation between the extent of intratetrahedral Y–O coordination and glass solubility can also be expected.[54]

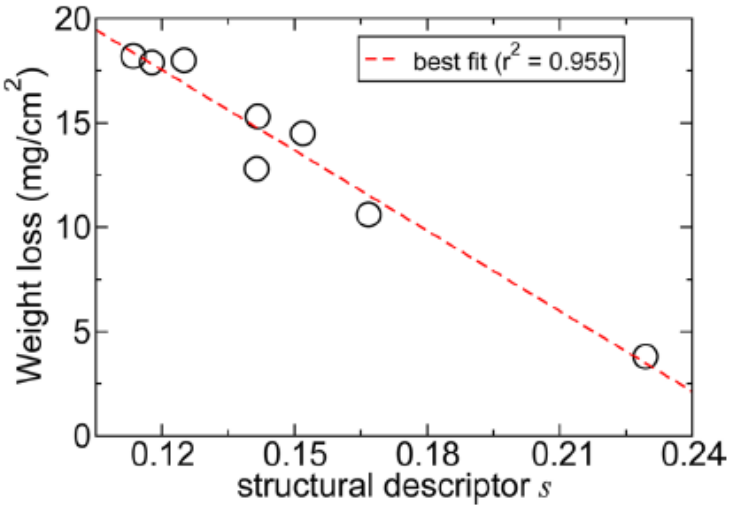

Figure 5. Correlation between Weight loss and the structural descriptor *s*. reprinted with permission from ref. 54 (to which refer for details). Copyright 2009 American chemical Society

The linear combination of these parameters *s* is given as:

$$s = 0.310\ CN_{SiOSi} + 0.076\ R_{Y\text{-}Y} - 0.136\ N_{intra} \quad (4)$$

A good correlation between the solubility of the glasses in water (measured as weight loss) and the descriptor *s* (Figure 5) is obtained, the correlation coefficients being $R^2 = 0.955$ ($\sigma = 0.97$ mg/cm^2). The negative slope of the regression indicates that as *s* increases, the solubility of the glass decreases. The coefficients of the first two terms of *s* are positive, implying that increasing the (Si−)O–Si coordination number and/or increasing the Y–Y clustering ratio will lead to decreasing solubility. Conversely, the sign of the third term of *s* is negative, implying that an increase in the number of intratetrahedral O–Si–O bonds around the yttrium atoms will increase the solubility.

It is worth noting that the R^2 statistical parameter for the correlation between the solubility *s* and the CN_{SiOSi} is 0.909 ($\sigma = 1.38$ mg/cm^2), denoting that CN_{SiOSi} captures most of the experimental trends; the observed small improvement in the linear fit for its combinations with other parameters in part arises from the larger number of parameters in the fit (overfitting).

3.4 QSPR models for Young's modulus

Elastic properties, specifically Young's modulus E, have attained paramount interest for a variety of glass applications such as accelerated devices, including hard discs and surgery equipment, lightweight construction, and composite materials.[46]

From a practical point of view, the mechanical properties of a glass often dictate whether a specific need or application can be met. Therefore, the prediction of these properties according to glass composition is becoming increasingly indispensable.

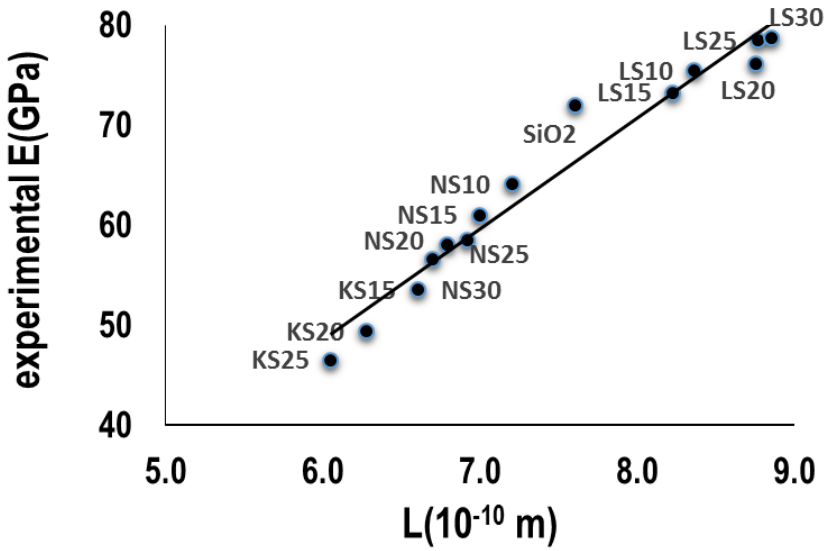

Figure 6. Correlation between the calculated Young's modulus (E) and the correlation length (L) of the first sharp diffraction peak of alkali silicate glasses. The plots is reproduced by the data values reported in ref. [56].

An interesting computational investigations on composition dependence of mechanical properties of multicomponent glasses has been performed by Pedone et al.[56, 57] This work represents the first detailed systematic computational study of the mechanical properties of three wide series of alkali silicate glasses, of general formula $x M_2O$-(100-x)SiO_2 (M=Li, Na, K; x=0, 10, 15, 20, 25, 30 mol%, obtained by means of the MD and energy minimization methods. Besides the correct quantitative calculations of the observable values of the mechanical properties (Young's modulus, shear modulus, bulk modulus and Poisson's ratio), the authors reported an important QSPR model between Young's modulus (E) and the correlation length (L) of the first sharp diffraction peak (FSDP).

Changes in the FSDP as a function of composition have been attributed to variation in the medium range order of the glass.[58] The quantitative rationalization of the Young's modulus modulation by dopant addition reported in Figure 6 promotes the correlation length as an eligible descriptor both for quantitative predictions and interpretation of the structure dependence of the Young's modulus for the alkali silicate glasses. Since the experimental Young's modulus values are reproduced by computational simulations with maximal differences of 4%, 4% and 2% for lithium, sodium and potassium silicate glasses, the statistical significance of the correlations obtained is comparable when experimental or computed Young's modulus data values are used: E(GPa)(Exp) =

10.993 L + 16.409 n = 14 R^2 = 0.932 S = 3.025; E(GPa)(Comput.) = 11.177 L + 18.654 n = 16 R^2 = 0.968 S = 2.191. It is worth noting the positive slope and the distribution of the glasses in the E-L space according to the nature of the dopant: the characteristic correlation length decreases as a function of Na and K content, and increases as a function of Li content. Therefore, the intermediate range order decreases with Na and K concentration, whereas the high field strength of Li determine the ordering of the surrounding network and modifier regions.

3.5 QSPR models for NMR spectra

Solid State nuclear magnetic resonance NMR spectroscopy has been firmly established as a powerful technique for glass structure investigation [60, 61], being very sensitive to the local environment (i.e., bond distances and angles, coordination numbers) and to the nature of the second coordination sphere. Unfortunately, the interpretation of the experimental spectra is hindered by the inhomogeneous broadening of isotropic line due to the different structural units present in the glass.

In the past the interpretation of the NMR spectra was based on empirical correlations derived from the study of crystalline materials with known structure,[62] and, successively, on correlations with structural descriptors computed by *ab-initio* calculations on crystals or model clusters. [63-68] However, crystalline systems generally exhibit a limited diversity of local structures in contrast to the disorder and variety of structural units (different coordination numbers and Q^n distributions) present in multicomponent glasses, and the cluster approach does not account for the correlations between structural factors that exist in solids and disorder in glasses.[69-71]

To overcome these limitations several studies focused on semi-quantitative comparisons between information derived from NMR spectra and structural features obtained from molecular dynamics simulations on large glass samples have been published. They mainly make use of connectivity between different types of Q^n species and related descriptors,[72-80] but attempts to investigate cation distribution and clustering have also been made.[81] Moreover, the interpretative and predictive relevance of statistical correlations between NMR-derived and MD-derived descriptors (quantitative structure-properties relationships) has also been discussed.[25, 33]

A major breakthrough occurred in the early 2000, when the calculation of NMR parameters from first principles [82] and, successively, the simulation of the line widths and shapes of the NMR spectra have become possible, [83-85] through the MD-DFT/GIPAW (Gauge Including Projector Augmented Wave) approach. This approach has opened a new route for interpreting NMR parameter distributions and for refining the relationships between NMR parameters and local structural features. In fact, calculations of NMR parameters (chemical shielding and quadrupolar parameters) of each nucleus is performed on the three-

dimensional model of the glass obtained by MD simulations and refined by Density Functional Theory (DFT) calculations. Then comparison between experimental and theoretical spectra features is performed, and, being the results satisfactory, the establishment of quantitative structure-NMR parameter relationships is feasible. Accurate relationships between NMR parameters and structural descriptors are extremely useful for the interpretation of experimental data, as they make a reverse approach possible. [83, 86-88] In this way, structural descriptors (i.e. bond and angle distributions) of a glass sample could, in principle, be directly obtained from the experimental NMR parameters distribution. (Figure 7)

Some examples of QSPR results involving NMR computed parameters and structural descriptors obtained by MD obtained for a number of multicomponent silicate glasses are summarized in **Table 1.**

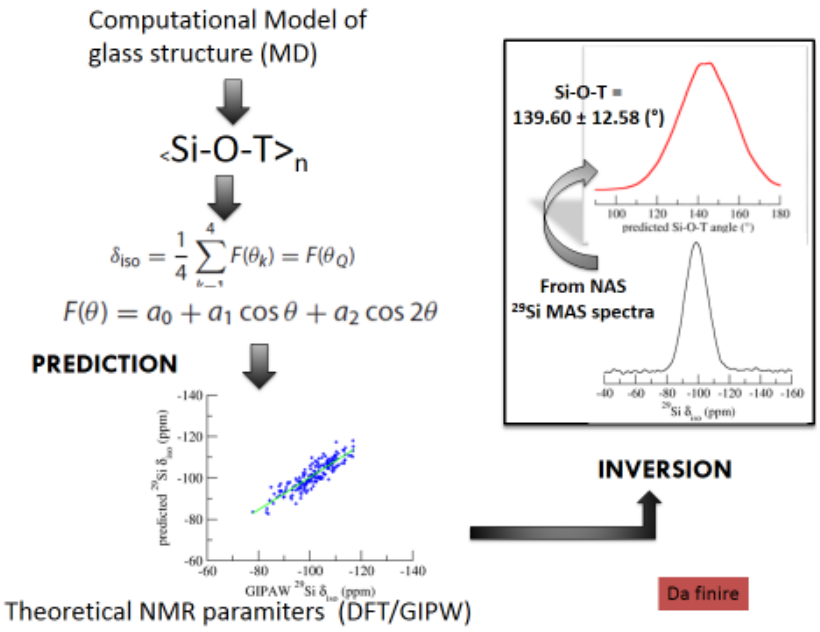

Figure 7. The structural inversion QSPR approach to extract structural distributions from NMR data. The example of the Si-O-T distribution for Sodium silicate glasses ig given.[86]

Direct information on structural regions dominated by different Q^n species in Alkaline/alkaline earth silicate glasses have been obtained from linear and multilinear regressions. The statistical models achieved an accuracy in prediction of about 2 ppm for the ^{29}Si δ_{iso},[86]10 ppm for the ^{23}Na δ_{iso},[90] of 2–4° for the

mean value of the Si-O-Si bond angle distribution, 2–4°,[86] and of less than 10 ppm for the chemical shift anisotropy $^{29}Si\ \Delta_{cs}$ of the Q^3 species.[90]

Two of the most investigated relationships in aluminosilicate glasses are those between ^{27}Al and $^{29}Si\ \delta_{iso}$ and inter-tetrahedral angles. (83, 95-97) In general poor correlations are obtained unless the connectivity between Si and Al and the different oxygen species (BOs, NBOs, TBOs) is taken into account. [93]

In the cases of phosphosilicate glasses (Bioglasses), the analysis of the correlation coefficients obtained for the linear correlations between the theoretical $^{29}Si\ \delta_{iso}$ and the mean Si−O−T angle (R^2 0.55, 0.62, and 0.89 for Q^1, Q^2, and Q^3 Si species, respectively) clearly indicates that the Q^n distribution of the Si species is controlled by the nonrandom distribution of Na and Ca atoms in the glass. [88, 94] The worst correlations coefficients have to be ascribed to the irregular distributions of Ca ions around the different Si Q^n species (its concentration is maximal around the Q^2 and minimal around the Q^4 species). This is a general trend which has been observed in alkaline and alkaline-earth glasses and aluminosilicate glasses.[84, 98]

Table 1. QSPR models of multicomponent silicate glasses involving NMR computed parameters and structural descriptors obtained by MD.

Glasses	NMR parameters	MD structural descriptors
Alkaline/alkaline earth silicate [84, 86, 88- 91]	$^{29}Si\ \delta_{iso}$ of each Q^n species	mean Si-O-T angle (T denotes the Q^n connected tetrahedron)
	$^{29}Si\ \Delta_{cs}$ of Q^3 species	<Si-O>BO and <Si-O>NBO bond lengths
	$^{17}O\ \delta_{iso}$ of BO and NBO	average Si-BO, Si-NBO and M-BO, N-NBO distances (M=Na,Ca)
	$^{23}Na\ \delta_{iso}$	number of coordinating NBO atoms to a given Na, mean Na-O bond length
Alumino silicate [79, 88, 91, 92]	^{27}Al and $^{29}Si\ \delta_{iso}$	<Al-O-T> and <Si-O-T> bond angles
	$^{29}Si\ \delta_{iso}$	amount of modifier cations in the silicon second coordination sphere
	$^{27}Al\ \delta_{iso}$	the fractional population of Al polyhedra
Phospho silicate (Bioglasses) [33, 88, 94]	^{29}Si NMR δ_{iso} of each Q^n species	mean Si−O−T angle
Boro silicate [87, 88]	^{29}Si and $^{11}B\ \delta_{iso}$	mean Si−O−T angle

Finally, an elegant example of structural inverse correlations is reported by Soleilhavoup et al.,[87] for borosilicate glasses. The methodology, derived for the first time for vitreous silica,[83] consists in extracting the distribution of NMR parameters (i.e. the distribution of isotropic chemical shifts for each boron resonance) from ^{11}B 3QMAS spectra; establishing a quantitative relationship between the ^{11}B isotropic chemical shift and each B–O–B angle; and mapping the NMR parameter distribution into a distribution of the B–O–B angle (structural inversion of the ^{11}B NMR spectrum).

4. Outlook

The main goal of computational material design is to gain "rational" control of the structure of complex real-life systems at all relevant length scales, thus the optimization and prediction of specific properties which fulfil end-user application requirements become possible. Notwithstanding the great advances achieved in computation, glass design is still in its infancy and constitutes an important avenue for future research.

To this respect, QSPR is a precious tool since it can be used at different steps of the problem-solving strategy for glass design: a) in a preliminary step, to assist end-users in the choice of the hierarchic level of theory and simulations to provide the most comprehensive description of the glass system at hand; b) in an intermediate steps, to map the amount of information derived from the computations to the space of the glass relevant properties. This might be devised to obtain the correct esteem of the numerical value of the property or to discover connections, trends and relationships that would otherwise be very difficult to detect by simple observation, i.e. to create a chemical model that is easy to understand; and c) at the final step to predict properties of new glass formulations in a cheap, efficient and environmentally friendly manner.

Such ambitious tasks require the development of improved atomistic simulation methods and/or new mathematical approaches that enable the quick derivation of specific descriptors for non-covalent amorphous systems at low computational costs.

For the time being, combination of MD and QSPR analysis helps to gain valuable information for the understanding of materials and chemical processes and furnishes a useful tool for predictive purposes.

References

1. A. Eugen, Glasses as engineering materials: A review, *Mater. Des.*, 2011, **32**, 1717-1732.
2. I. Izquierdo-Barba, A.J. Salinas, M. Vallet-Regi, M Bioactive Glasses: From Macro to Nano. *Int. J. App. Glass Sci*., 2013, **4**, 149-161.

3. J. Hum, A.R. Boccaccini, Bioactive glasses as carriers for bioactive molecules and therapeutic drugs: a review, J. Mater. Sci. – Mater. M., 2012, 23, 2317-2333.
4. G. N. Greaves and S. Sen, Inorganic glasses, glass-forming liquids and amorphizing solids, *Adv. Phys.*, 2007, **56**, 1-166.
5. SciGlass 6.5 Database and Information System, 2005. http://www.sciglass.info/
6. International Glass Database System Interglad Ver.7; http://www.newglass.jp/interglad_n/gaiyo/info_e.html)
7. A. I. Priven, O.V. Mazurin, Glass property databases: Their history, present state, and prospects for further development. Glass - The Challange for the 21st Century-*Adv. Mat. Res*., 2008, **39-40**, 147-152.
8. A. I. Priven, General method for calculating the properties of oxide glasses and glass forming melts from their composition and temperature, *Glass Technol.*, 2004, **45**, 244-254.
9. A. Pedone, G. Malavasi, M. C. Menziani, A. N. Cormack and U. Segre, A New Self-Consistent Empirical Interatomic Potential Model for Oxides, Silicates, and Silica Based Glasses, J. Phys. Chem. B, 2006, 110, 11780-11795.
10. A. Tilocca, N. de Leeuw and A. N. Cormack, Shell-model molecular dynamics calculations of modified silicate glasses, Phys. Rev. B, 2006, 73, 104209-104223.
11. A. Pedone, M. Corno, B. Civalleri, G. Malavasi, M.C. Menziani, U. Segre, P. Ugliengo, An ab initio parameterized interatomic force field for hydroxyapatite. *J. Mat. Chem*., 2007, **17**, 2061-2068.
12. A. Pedone, G. Malavasi, M.C. Menziani, U. Segre, F. Musso, M. Corno, B. Civalleri, P. Ugliengo, FFSiOH: a New Force Field for Silica Polymorphs and Their Hydroxylated Surfaces Based on Periodic B3LYP Calculations. *Chem. Mater.,* 2008, **20**, 2522-2531.
13. A. Tilocca, Short- and medium-range structure of multicomponent bioactive glasses and melts: An assessment of the performances of shell-model and rigid-ion potentials J. Chem. Phys., 2008, 129, 084504.
14. M. Salanne, B. Rotenberg, S. Jahn, R. Vuilleumier, C. Simon and P. A. Madden, Including many-body effects in models for ionic liquids, Theor. Chem. Acc., 2012, 131, 1143-1149.
15. A. Pedone, Properties Calculations of Silica-Based Glasses by Atomistic Simulations Techniques: A Review, J. Phys. Chem. C, 2009, 113, 20773-20784.
16. M. E. Eberhart, D. P. Clougherty. Looking for design in material design. *Nature Materials*, 2004, **3**, 659-861.
17. K. Wu, B. Natarajan,L. Morkowchuk, M. Krein, C. M. Breneman, From drug discovery QSAR to predictive materials QSPR: the evolution of descriptors, methods, and models. pp. 385-410 in Informatics dor materials science and engineering, K. Rajan, Ed., Amsterdam, Elsevier, 2013.
18. A. R. Katritzky, U. Maran, V. S. Lobanov, M. Karelson. Structurally Diverse Quantitative Structure-Property Relationship Correlations of

Technologically Relevant Physical Properties. *J. Chem. Inf. Comput. Sci*., 2000, **40**, 1-18.
19. W. M. Berhanu, G.G. Pillai, A. A. Oliferenko, A. R. Katritzky, Quantitative Structure-Activity/Property Relationships: The Ubiquitous Links between Cause and Effect. *ChemPlusChem*. 2012, **77**, 507-517.
20. A. R. Katritzky, M. Kuanar, S. Slavov, C. D. Hall, M. Karelson, I Kahn, D. A. Dobchev, Quantitative Correlation of Physical and Chemical Properties with Chemical Structure: Utility for Prediction., *Chem. Rev*., 2010, **110**, 5714-5789
21. T. Le, V.C. Epa, F.R. Burden, D. A.Winkler, Quantitative Structure-Property Relationship Modeling of Diverse Materials Properties, *Chem Rev.*, 2012, **112**, 2889-2919.
22. M. Karelson, V. S. Lobanov, A. R. Katritzky, Quantum-chemical descriptors in QSAR/QSPR studies. *Chem. Rev*., 1996, **96**, 1027-1043.
23. G. S. Henderson, The structure of silicate melts: A glass perspective. *Can. Mineral*., 2005, **43**, 1921-1958.
24. G. Mountjoy, B. M. Al-Hasni and C. Storey, Structural organisation in oxide glasses from molecular dynamics modeling *J. Non-Cryst Solids*, 2011, **357**, 2522-2529.
25. G. Malavasi, A. Pedone, M.C. Menziani Towards a quantitative rationalization of multicomponent glass properties by means of Molecular Dynamics simulations, *Mol. Sim.* 2006, **32**, 1045-1055, 2006.
26. L. Adkins, A. N. Cormack, Large-scale simulations of sodium silicate glasses *J. Non-Cryst. Solids*, 2011, **357**, 2538-2541.
27. G. Malavasi, M. C. Menziani, A. Pedone, U. Segre, Void size distribution in MD-modelled silica glass structures, *J. Non-Cryst. Solids*, 2006, **352**, 285-296.
28. P. X. Liu, W. Long, Current mathematical methods used in QSAR/QSPR Studies Int. J. Mol. Sci. 2009, 10, 1978 – 1998.
29. K. Baumann, Cross-validation as the objective function for variable-selection techniques. TrAC, Trends in Anal. Chem., 2003, 22, 395-406.
30. S. Inabaw, S. Fujino, Empirical Equation for Calculating the Density of Oxide Glasses, *J Am. Ceram. Soc.*, 2010, **93**, 217-220.
31. M. B. Volf, Mathematical Approach to Glass; Glass Science and Technology, vol. 9. Elsevier, Prague, 1988; and references therein.
32. I. Priven, O. V. Mazurin, Comparison of Methods Used for the Calculation of Density, Refractive Index and Thermal Expansion of Oxide Glasses, *Glass Technol*., 2003, **44**, 156–66.
33. L. L. Linati, G.; Malavasi, G.; Menabue, L.; Menziani, M. C.; Mustarelli, P.; Segre, U., Qualitative and quantitative Structure-Property Relationships (QSPR) analysis of multicomponent potential bioglasses, *J. Phys. Chem. B*, 2005, **109**, 4989-4998.
34. G. Lusvardi, G. Malavasi, L. Menabue, M. C. Menziani, A. Pedone, U. Segre, Density of multicomponent silica-based potential bioglasses: Quantitative

structure-property relationships (QSPR) analysis. *J. Eur. Ceram. Soc.*, 2007, **27**, 499-504.
35. A. I. Priven, Evaluation of the fraction of fourfold-coordinated boron in oxide glasses from their composition. *Glass Phys. Chem*., 2000, **26**, 441-454.
36. L. I. Demkina Investigation of the dependence of glass properties on their composition. *Izd. Chimia*, 1976, **23**, 123-127.
37. G. Lusvardi, G. Malavasi, F. Tarsitano, L., Menabue, M.C. Menziani, A. Pedone, Quantitative Structure-Properties Relationships of Potentially Bioactive Fluoro Phospho-Silicate Glasses. *J. Phys. Chem. B*, 2009, **113**, 10331–10338.
38. G. Lusvardi, G. Malavasi, M. Contrada, L., Menabue, M.C. Menziani, A. Pedone, U. Segre, Elucidation of the structural role of fluorine in potentially bioactive glasses by experimental and computational investigation, *J. Phys. Chem. B*, 2008, **112**, 12730-12739.
39. L. L. Hench, Bioactive materials: the potential for tissue generation, *Biomaterials*, 1998, **19**, 1419-1423.
40. J. E. Shelby,. Introduction to Glass Science and Technology; RCS Paperbacks, Cambridge, UK, 1997.
41. G. Engelhardt, D. Michel, High-Resolution Solids State NMR of Silicate and Zeolites; Wiley & Son, Chichester, UK, 1987.
42. G. N. Greaves, S. Sen, Inorganic Glasses, Glass-Forming Liquids and Amorphising Solids. *Adv. Phys*. 2007, *56*, 1-166.
43. K. Christie, A. Pedone, M. C. Menziani, A. Tilocca, Fluorine Environment in Bioactive Glasses: ab Initio Molecular Dynamics Simulations, *J. Phys. Chem. B*, 2011, **115**, 2038-2045.
44. A. Pedone, T. Charpentier, M.C. Menziani, The structure of fluoride-containing bioactive glasses: new insights from first-principles calculations and solid state NMR spectroscopy, *J. Mater. Chem*., 2012, **22**, 12599-12608.
45. J. A. Kerr, CRC Handbook of Chemistry and Physics 1999-2000: A Ready-Reference Book of Chemical and Physical Data; D.R. Lide (Ed.), CRC Press, Boca Raton, Florida, USA, 81st edition, 2000.
46. L. Wondraczek1, J. C. Mauro, J. Eckert, U. Kühn, J. Horbach, J. Deubener, T. Rouxel, Towards Ultrastrong Glasses, *Adv. Mat.*, 2011, **23**, 4578-4586.
47. L. L. Hench, D. E. Day, W. Höland, V. M. Rheinberger, Glass and Medicine, *Int. J. App. Glass Sci*., 2010, **1**,104-117.
48. T. Kokubo, An introduction to bioceramics. In Advanced Series in Ceramics. L.L. Hench, J. Wilson (Ed.)., World Scientific Publishing Co., Singapore (1993). Vol.1.
49. M. Brink, T. Turunen, R.P. Happonen, A. Yli-Urpo. Compositional dependence of bioactivity of glasses in the system Na_2O-K_2O-MgO-CaO-B_2O_3-P_2O_5-SiO_2. *J. Biomed. Mater. Res*., 1997, **37**, 114-121.
50. G. Lusvardi, G. Malavasi, L. Menabue, M. C. Menziani Synthesis, characterization and molecular dynamics simulation of Na_2O-CaO-SiO_2-ZnO glasses. *J. Phys. Chem. B*, 2002, **106**, 9753-9760.

51. G. Lusvardi, G. Malavasi, A. Pedone, L. Menabue, M. C. Menziani,V. Aina, A. Perardi, C. Morterra, F. Boccafoschi, S. Gatti, M. Bosetti , M. F. Cannas Properties of Zinc Releasing Surfaces for Clinical Applications *J. Biomater. Appl*., **22**, 505-526, 2008.
52. G. Lusvardi, G. Malavasi, L. Menabue, M. C. Menziani, A combined experimental-computational strategy for the design, synthesis and characterization of bioactive zinc-silicate glasses. *Key Engineering Materials*, 2008, **377**, 211-224.
53. G. Lusvardi, D. Zaffe, L. Menabue, C. Bertoli, G. Malavasi, U. Consolo, In vitro and in vivo behaviour of zinc-doped phosphosilicate glasses, *Acta Biomater*., 2009, **5**, 419-428.
54. J. K. Christie, A. Tilocca, Molecular Dynamics Simulations and Structural Descriptors of Radioisotope Glass Vectors for In Situ Radiotherapy *J. Phys. Chem. B*, 2012, **116**, 12614–12620.
55. A. Tilocca, A. N. Cormack , N. H. de Leeuw The Structure of Bioactive Silicate Glasses: New Insight from Molecular Dynamics Simulations, *Chem. Mater.*, 2007, **19**, 95–103.
56. A. Pedone, G. Malavasi, A. N. Cormack, U. Segre, M. C. Menziani, Insight into elastic properties of binary alkali-silicate glasses; prediction and interpretation through atomistic simulation techniques. *Chem. Mater*., 2007, **19**, 3144-3154.
58. A. Pedone, G. Malavasi, A. N. Cormack, U. Segre, M. C. Menziani Elastic and dynamical properties of silicate glasses from computer simulations techniques. *Theor. Chem. Acc*., 2008, **120**, 557-564.
59. G. Hauret, Y. Vaills, T. Parot-Rajaona, F. Gervais, D. Mas, Y. Luspin, J. Dynamic behaviour of (1−x) SiO2-0.5xM2O glasses (M = Na, Li) investigated by infrared and Brillouin spectroscopies, *Non-Cryst. Solids*, 1995, **191**, 85-93.
60. M. Eden, NMR studies of oxide-based glasses, *Annu. Rep. Prog. Chem., Sect. C: Phys. Chem*, 2012, **108**, 177-221.
61. J. V. Hanna, M. E. Smith, Recent technique developments and applications of solid state NMR in characterising inorganic materials. *Solid State NMR*, 2010, **38**, 1-18.
62. G. Engelhardt, D. Michel, High-Resolution Solid-State Nmr of Silicates and Zeolites 1988, John Wiley & Sons Inc.
63. J. A. Tossell, P. Lazzeretti, Abinitio Calculations of Oxygen Nuclear-Quadrupole Coupling Constants and Oxygen and Silicon NMR Shielding Constants in Molecules Containing Si-O Bonds, *Chem. Phys.*, 1987, **112**, 205-212.
64. J. A. Tossell, Calculation of NMR Shieldings and other Properties for 3 and 5 coordinate Si, 3 coordinate-O and some Siloxane and Boroxol Ring Compounds, *J Non-Cryst Solids*, 1990, **120**, 13-19.
65. X. Xue, M. Kanzaki, An ab initio calculation of ^{17}O and ^{29}Si NMR parameters for SiO_2 polymorphs, *Solid State Nucl. Magn. Reson.*, 2000, **16**, 245-259.

66. T. Clark, P. J. Grandinetti, P. Florian, J. F. Stebbins, An ^{17}O NMR investigation of crystalline sodium metasilicate: implications for the determination of local structure in alkali silicates, *J. Phys. Chem.*, 2001, **105**, 12257-12265.
67. H. Maekawa, P. Florian, D. Massiot, H. Kiyono and M. Nakaruma, Effect of alkali metal oxide on ^{17}O NMR parameters and Si-O-Si angles of alkali metal disilicate glasses, *J. Phys. Chem.*, 1996, **100**, 5525-5532.
68. J. A. Tossell, Quantum mechanical calculation of ^{23}Na NMR shieldings in silicates and aluminosilicates, *Phys Chem Minerals*, 1999, **27**, 70-80.
69. A. Pedone, M. Biczysko, V. Barone, Environmental Effects in Computational Spectroscopy, *ChemPhysChem*, 2010, **11**, 1812-1832.
70. A. Pedone, M. Pavone, M. C. Menziani, V. Barone, Accurate First-Principle Prediction of ^{29}Si and ^{17}O NMR Parameters in SiO_2 Polymorphs: The Cases of Zeolites Sigma-2 and Ferrierite, *J. Chem. Theory and Computation*, 2008, **4**, 2130-2140.
71. J. Casanovas, F. Illas, G. Pacchioni, Ab initio calculations of ^{29}Si solid state NMR chemical shifts of silcane and silanol groups in silica, *Chem. Phys. Lett.*, 2000, **326**, 523-529.
72. L. Linati, G. Lusvardi, G. Malavasi, L. Menabue, M. C. Menziani, P. Mustarelli, A. Pedone, U. Segre, Medium range order in phospho-silicate bioactive glasses: insights from MAS-NMR spectra, Chemical durability experiments and Molecular Dynamics Simulations, *J. Non-Cryst. Solids*, 2008, **354**, 84-89.
73. J. A. Tossell, J. Horbach, O triclusters revisited: classical MD and quantum cluster results for glasses of composition $(Al_2O_3)2(SiO_2)$. *J. Phys. Chem. B*, 2005, **109**, 1794-1797.
74. L. Olivier, X. Yuan, A. N. Cormack, C. Jäger, Combined 29Si double quantum NMR and MD simulation studies of network connectivities of binary $Na_2O•SiO_2$ glasses: new prospects and problems, *J. Non-Cryst Solids*, 2001, **293-295**, 53-66.
75. C. Leonelli, G. Lusvardi, M. Montorsi, M. C. Menziani, L. Menabue, P. Mustarelli, L. Linati, Influence of small additions of Al_2O_3 on the properties of the $Na_2O•3SiO_2$ glass, *J. Phys. Chem. B*, 2001, **105**, 919-927.
74. B. Park, H. Li, L. R. Corrales, Molecular dynamics simulation of La_2O_3-Na_2O-SiO_2 glasses. II. The clustering of La^{3+} cations, *J. Non-Cryst Solids*, 2002, **297**, 220-238.
75. L. Barbieri, V. Cannillo, C. Leonelli, M. Montorsi, C. Siligardi, P. Mustarelli, Characterisation of CaO-ZrO_2-SiO_2 glasses by MAS-NMR and molecular dynamics *Phys. Chem. Glasses-B*, 2004, **45**, 138-140.76. E. Kashchieva, B. Shivachev, Y. Dimitriev, Molecular dynamics studies of vitreous boron oxide, *J. Non-Cryst Solids*, 2005, **351**, 1158-1161.
77. J. Machacek, O. Gedeon and M. Liska, Group connectivity in binary silicate glasses, *J. Non-Cryst Solids*, 2006, **352**, 2173-2179.

78. G. Mountjoy, B. M. Al-Hasni, C. Storey, Structural organisation in oxide glasses from molecular dynamics modeling *J Non-Cryst Solids*, 2011, **357**, 2522-2529.
79. A. Jaworski, B. Stevensson, B. Pahari, K. Okhotnikov, M. Eden, Local Structures and Al/Si Ordering in Lanthanum Aluminosilicate Glasses Explored by Advanced ^{27}Al NMR Experiments and Molecular Dynamics Simulations *Phys. Chem. Chem. Phys.*, 2012, **14**, 15866-15878.
80. H. Inoue, A. Masuno, T. Watanabe, Modeling of the structure of sodium borosilicate glasses using pair potentials, *J. Phys. Chem. B*, 2012, **116**, 12325-12331.
81. U. Voigt, H. Lammert, H. Eckert, A. Heuer, Cation clustering in lithium silicate glasses: Quantitative description by solid-state NMR and molecular dynamics simulations *Phys. Rev. B*, 2005, **72**, 64207
82. C. J. Pickard, F. Mauri, All-electron magnetic response with pseudopotentials: NMR chemical shifts, *Phys. Rev. B*, 2001, **63**, 245101
83. T. Charpentier, P. Kroll, F. Mauri, First-Principles Nuclear Magnetic Resonance Structural Analysis of Vitreous Silica, *J. Phys. Chem. C*, 2009, **113**, 7917-7929.
84. A. Pedone, T. Charpentier, M. C. Menziani, Multinuclear NMR of $CaSiO_3$ glass: simulation from first-principles, *Phys. Chem. Chem. Phys.*, 2010, **12**, 6054-6066.
85. T. Charpentier, The PAW/GIPAW approach for computing NMR parameters: A new dimension added to NMR study of solids, *Solid State Nucl. Magn. Reson.*, 2011, **40**, 1-20.
86. F. Angeli, O. Villain, S. Schuller, S. Ispas, T. Charpentier, Insight into sodium silicate glass structural organization by multinuclear NMR combined with first-principles calculations, *Geochim. Cosmochim. Acta*, 2011, **75**, 2553-2469.
87. A. Soleilhavoup, J.-M. Delaye, F. Angeli, D. Caurant, T. Charpentier, Contribution of first-principles calculations to multinuclear NMR analysis of borosilicate glasses, *Magn. Res. Chem.*, 2010, **48**, S159-S170.
88. T. Charpentier, M. C. Menziani, A. Pedone, Computational simulations of solid state NMR spectra: a new era in structure determination of oxide glasses. *RSC Adv*., 2013, **3**, 10550-10578.
89. S. Ispas, T. Charpentier, F. Mauri, D. R. Neuville, Structural properties of lithium and sodium tetrasilicate glasses: Molecular dynamics simulations versus NMR experimental and first-principles data *Solid State Sci.*, 2010, **12**, 183-192.
90. T. Charpentier, S. Ispas, M. Profeta, F. Mauri, C. J. Pickard, First-principles calculation of ^{17}O, ^{29}Si, and ^{23}Na NMR spectra of sodium silicate crystals, *J. Phys. Chem. B*, 2004, **108**, 4147-4161.
91. A. Pedone, E. Gambuzzi, M. C. Menziani, Unambiguous Description of the Oxygen Environment in Multicomponent Aluminosilicate Glasses from ^{17}O Solid State NMR Computational Spectroscopy, *J. Phys. Chem. C*, 2012, **115**, 14599-14609.

92. A. Pedone, E. Gambuzzi, G. Malavasi, M. C. Menziani, First-Principles Simulations of the ^{27}Al and ^{17}O Solid State NMR spectra of a calcium alumino-silicate glass, *Theor. Chem. Acc.*, 2012, **131**, 1147-1157.
93. E. Gambuzzi, A. Pedone, M. C. Menziani, F. Angeli, D. Caurant, T. Charpentier, Probing silicon and aluminium chemical environments in silicate and aluminosilicate glasses by solid state NMR spectroscopy and accurate first-principles calculations, *Geochim. Cosmochim. Acta*, in press.
94. A. Pedone, T. Charpentier, G. Malavasi, M. C. Menziani, New Insights into the Atomic Structure of 45S5 Bioglass by Means of Solid-State NMR Spectroscopy and Accurate First-Principles Simulations, *Chem. Mater.*, 2010, **22**, 5644-5652.
95. F. Angeli, J. M. Delaye, T. Charpentier, J. C. Petit, D. Ghaleb, P. Faucon, Investigation of Al–O–Si bond angle in glass by ^{27}Al 3Q-MAS NMR and molecular dynamics. *Chem. Phys. Lett.*, 2000, **320**, 681-687.
96. E. Lippmaa, A. Samoson, M. Magi High-Resolution ^{27}Al NMR of Aluminosilicates *J. Am. Chem. Soc.*, 1986, **108**, 1730-1735.
97. F. Mauri, A. Pasquarello, B. G. Pfrommer, Y. G. Yoon, S. G. Louie Si-O-Si bond-angle distribution in vitreous silica from first-principles ^{29}Si NMR analysis. *Phys. Rev. B*, 2000, **62**, R4786-R4789.
98. P. Florian, F. Fayon, D. Massiot, 2J Si−O−Si Scalar Spin−Spin Coupling in the Solid State: Crystalline and Glassy Wollastonite $CaSiO_3$. *J. Phys. Chem. C*, 2009, **113**, 2562-2572.